

Starburst Galaxies Under the Microscope: High-Resolution Observations with VISIR and SINFONI

Paul P. van der Werf, Leonie Snijders,
Liesbeth Vermaas, Juha Reunanen and
Marten Hamelink (Leiden Observatory,
the Netherlands)

Infrared observations of starburst galaxies not only enable penetration of the obscuring veil of dust, but also provide unique diagnostics in the form of nebular emission lines and emission from dust and polycyclic aromatic hydrocarbons (PAHs). Here we describe some first results of our ongoing study of starburst galaxies with VISIR and SINFONI at the VLT.

Starburst galaxies

Starburst galaxies are unique laboratories. Starburst episodes are phases in the evolution of galaxies that are by definition transient, and during which they convert a significant fraction of their gas reservoirs into stars. During a starburst phase a galaxy thus evolves rapidly in stellar, gas, dust and metal content, colour, luminosity and morphology. Starburst galaxies also cover an enormous range in luminosity. At the low luminosity end the small star-forming dwarf galaxies such as the Small and Large Magellanic Clouds have infrared luminosities $L_{\text{IR}} = 7 \cdot 10^7 L_{\odot}$ and $L_{\text{IR}} = 7 \cdot 10^8 L_{\odot}$. More distant infrared-bright dwarf galaxies typically have $L_{\text{IR}} = 3 \cdot 10^9 L_{\odot}$. Well-studied nearby starbursts such as NGC 253 and M82 have $L_{\text{IR}} = 3 \cdot 10^{10} L_{\odot}$ and $6 \cdot 10^{10} L_{\odot}$. At higher luminosities, we have the luminous infrared galaxies (LIRGs) with $L_{\text{IR}} > 10^{11} L_{\odot}$. (e.g., the Antennae, NGC 4038/4039), the ultraluminous infrared galaxies (ULIRGs) with $L_{\text{IR}} > 10^{12} L_{\odot}$ (e.g. Arp 220), and the hyperluminous infrared Galaxies (HyLIRGs) with $L_{\text{IR}} > 10^{13} L_{\odot}$. While the luminosity range spanned is more than five decades, the starbursts that are most amenable to detailed study are obviously the nearest ones, which have only moderate luminosity. It is therefore important to understand how these nearby starbursts relate to their more distant and spectacular cousins.

Since stars form in dusty molecular clouds, it is no surprise that (most) starbursts are also dusty. The study of starburst galaxies has therefore received

an enormous boost from technical developments in ground-based and space-based infrared astronomy. The infrared regime in fact offers two advantages. In the first place, reduced extinction offers the opportunity to see through the obscuring dust, and to probe the active star-forming complexes directly. Secondly, a number of unique diagnostics are available in the infrared in the form of highly diagnostic nebular emission lines, H_2 vibrational lines which provide a kinematic probe of the molecular gas at high spatial resolution, and emission and absorption features of the dust itself, including those attributed to polycyclic aromatic hydrocarbons (PAHs).

We have recently embarked on an observational study of nearby starbursts with two new VLT instruments: SINFONI and VISIR, and here report some first results.

The importance of spatial resolution

The study of starburst galaxies through infrared techniques has benefited significantly from observations with the Infrared Space Observatory (ISO) and the Spitzer Space Telescope. Yet, while these space-based observations have provided unmatched sensitivity and wavelength coverage, they cannot provide the spatial resolution enabled by ground-based telescopes. VISIR at the VLT has opened up the ground-based mid-infrared (mid-IR) spectral region for routine imaging and spectroscopy at an angular resolution of $0.3''$ (essentially the diffraction limit of the VLT). For comparison, the resolution of Spitzer at $8 \mu\text{m}$ is $2.5''$. Thus VISIR gains over Spitzer in spatial resolution by a factor of eight in two dimensions. As we will show, this gain in spatial resolution is fundamentally important for studying the anatomy of starburst galaxies in detail. The VISIR data are complemented with SINFONI near-infrared (near-IR) integral field spectroscopy at a similar resolution. High spatial resolution allows us to isolate active star-forming regions from diffuse extended emission and thus provides a more secure diagnostic of the conditions in the star-forming regions themselves (e.g., local densities and radiation fields). An application of this is the determination of the mass of the most massive star in a young star-forming re-

gion, for which the youngest regions have to be isolated. A second example is the origin of the PAH emission in starburst galaxies, which can be studied if the emission regions and the local sources of excitation can be spatially resolved. Both of these require high spatial resolution and will be discussed in some detail in the following sections.

A case study: superstarclusters in the Antennae (NGC 4038/4039)

The Antennae system (NGC 4038/4039) is the nearest major merger of two large spiral galaxies. Since the beginning of the interaction the system went through several episodes of violent star formation, of which the last one is probably still ongoing.

The resulting star clusters have been studied extensively. Radio and mid-IR observations show that the region between the two remnant nuclei (usually referred to as the overlap region) hosts spectacular obscured star formation. The brightest mid-IR component produces 15 % of the total $15 \mu\text{m}$ luminosity of the entire system (Mirabel et al. 1998). This region is covered by a prominent dust lane and may be associated with a faint, red source in Hubble Space Telescope (HST) images, illustrating how optical data alone are insufficient to identify and study the youngest star-forming regions. Such superstarclusters are of interest as potentially the youngest simple coeval stellar populations in starbursts and thus furnish excellent tests for the properties of the most massive stars formed in these systems. For sufficiently massive and young superstarclusters, they may offer the opportunity of directly measuring a possible upper mass cutoff of the stellar Initial Mass Function (IMF). Mid-IR nebular fine-structure lines are excellent probes of such systems, since they are relatively unaffected by dust and can be used to measure the temperature of the ionising radiation field, and hence the masses of the most massive stars present.

We used VISIR to study the most prominent clusters at $0.3''$ resolution (30 pc at the assumed distance of 21 Mpc for the Antennae). Our data set consists of

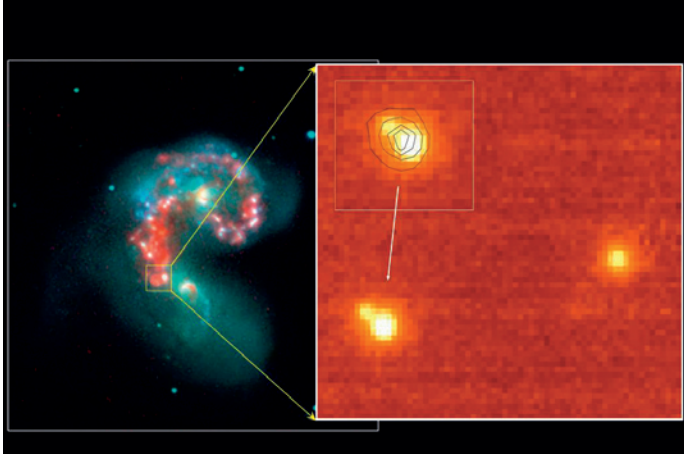
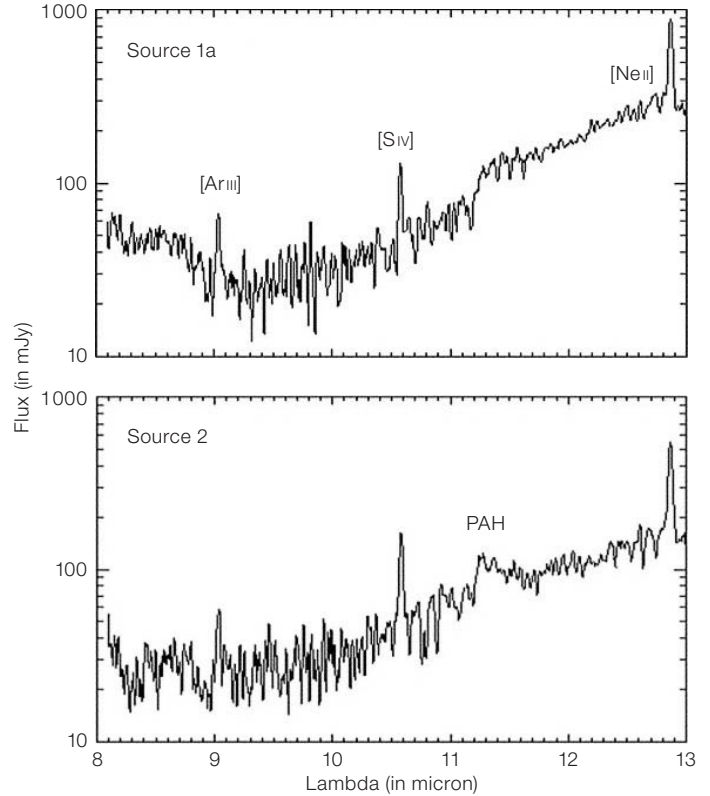


Figure 1 (above): VISIR image of the [Ne II] 12.8 μm emission from the most prominent superstarclusters in the Antennae (right panel). The diameter of the VISIR field shown here is 9". Its location is indicated in the left panel, which shows a composite of data obtained with Spitzer (Wang et al. 2004). The inset in the right panel shows the contours of the dust emission at 11.3 μm overlaid on the [Ne II] image (from Snijders et al. 2006).

Figure 2 (right): VISIR spectra, taken with a 0.75" slit, of the two prominent superstarclusters in the Antennae seen in Figure 1. Source 1a is the brightest part of the Eastern source, while Source 2 is the Western source. The apparently enhanced noise from 9 to 10 μm results from the log scale of these plots (from Snijders et al. 2006).



imaging in a number of narrow-band filters in the *N*-band, and long-slit spectroscopy with a 0.75" slit, covering the two most prominent clusters. Some key results are shown in Figures 1 and 2 (Snijders et al. 2006), which show a number of surprising results. In the first place, the Eastern cluster is separated into two components, separated by approximately 0.5" (50 pc). The brightest of these two (cluster 1a) is slightly resolved. This result immediately shows that any attempt to model this region as a single coeval stellar population is flawed. Cluster 1b has no counterpart in any other available data set; from the available upper limits, we derive a visual extinction $A_V > 72^m$ towards this cluster. Remarkably, the 11.3 μm emission shows a different morphology, suggesting a common envelope of emission from hot dust and polycyclic aromatic hydrocarbons (PAHs). Cluster 2, which is optically complex, is a simple and compact object at 10 μm ; presumably the *N*-band emission is dominated by a single (obscured) object within the general complex.

An even more surprising result comes from comparison with Spitzer-IRS spec-

tra (Brandl, priv. comm.) with a 5" slit, revealing that approximately 75 % of the 12 μm continuum is detected in the 0.75" VISIR slit; however, the equivalent width of the 11.3 μm PAH feature in the VISIR data is much smaller than in the larger aperture Spitzer spectra.

Both clusters exhibit emission in the 10.5 μm [S IV] line, an ionisation stage requiring 34.8 eV (while the 12.8 μm [Ne II] line requires only 21.6 eV); in particular in cluster 2 the [S IV]/[Ne II] ratio in our data is higher than in larger aperture Spitzer data, significantly affecting the interpretation of the results, and indicating that VISIR closes in on the regions of most intense star formation, while larger aperture data are significantly affected by more diffuse emission.

A detailed analysis of the fine-structure line ratios in the two clusters indicates conditions similar to those in Galactic ultracompact H II regions (but extended over tens of parsecs). This is an important result, since it would affect the interpretation of results at other wavelengths (from radio to near-IR) as well (Snijders et al., in preparation).

The low equivalent width of the PAH emission indicates that either the PAHs are destroyed in the direct environment of the superstarclusters, or that the PAH emission is not preferentially excited by the superstarclusters, but is dominated by more diffuse emission, excited by the softer UV radiation from more widespread young stars of slightly later type. Understanding which of these explanations is correct is important for the interpretation of the PAH emission. In order to study this issue further, we now turn to a more nearby starburst, where much higher linear resolution is obtained.

The resolved starburst in M83

M83 is a nearby ($D = 4.5$ Mpc) grand-design barred spiral with a nuclear region that is sometimes described as 'amorphous'. It has a prominent optical peak, which is however not at the centre of the fainter isophotes and therefore probably not the dynamical centre. The starburst in M83 is not centred on this optical peak, but displaced significantly towards the West. The situation is illustrated in Figure 3. Here the *K*-band continuum is

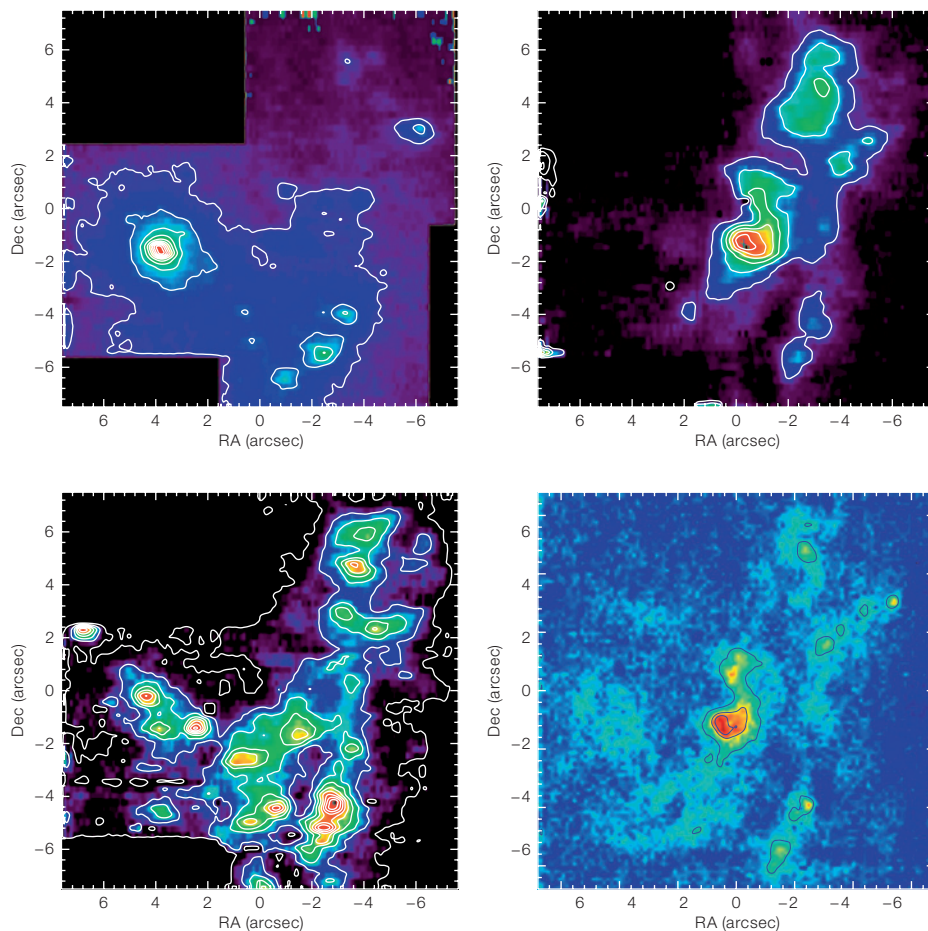


Figure 3: The off-nuclear starburst in M83. Each of these frames shows a $13.6'' \times 13.6''$ (300 pc diameter) region. **Top-left panel:** *K*-band continuum (from SINFONI); **top-right panel:** Br γ 2.17 μm (from SINFONI); **lower-left panel:** [FeII] 1.26 μm (from SINFONI). These data result from three overlapping SINFONI exposures, with on-source integration times of 10 minutes per frame and per spectral band (from Vermaas et al., in preparation); **lower-right panel:** 11.3 μm PAH emission obtained with VISIR (from Snijders et al., in preparation).

dominated by the underlying bulge population, with emission from red supergiants formed in the starburst superimposed. The full spectral data cubes produced by SINFONI provide a wealth of detail on the morphology and spatial and temporal evolution of this starburst, which is illustrated by the spectra shown in Figure 4.

Key spectral features which are evident in these spectra include lines of ionised hydrogen (Br γ 2.17 μm in the *K*-band, the Brackett series in the *H*-band and Pa β 1.28 μm in the *J*-band). These lines trace the distribution of the young massive stars (spectral types B3 and earlier) and (under the usual assumption of dust-free and ionisation-bounded HII regions) provide a direct measurement of the Lyman continuum output of these stars; in addition, combining these lines gives a direct measurement of the extinction towards the ionised gas. In addition we observe HeI lines (principally the 2.06 μm and 1.70 μm lines, but also fainter transi-

tions). These lines trace the helium-ionising continuum and therefore the most massive stellar population in the starburst. In principle helium/hydrogen recombination line ratios can be used to measure the relative volumes of the helium and hydrogen Strömgren spheres and thus the hardness of the ionising radiation field. In practice, collisional excitation effects from metastable levels in the helium atom make this procedure complicated, and in particular the use of the bright HeI 2.06 μm line is fraught with difficulties; however, the HeI 1.70 μm line is quite suitable for this purpose.

In addition we find forbidden fine-structure lines of singly ionised iron, principally the [FeII] 1.64 μm line in the *H*-band and the 1.26 μm line in the *J*-band. The [FeII] emission results from strong shocks from supernovae, which destroy the dust grains, thus raising the gas-phase iron abundance by a large factor. The resulting iron atoms are then easily ionised

and excited by the supernova blast wave shock. Since the [FeII] 1.64 μm and 1.26 μm lines originate from the same upper level, their intrinsic ratio is fixed and the observed line ratio can thus be used as an independent extinction measurement. Furthermore, fainter [FeII] lines can be used to constrain temperature and density of the emitting material.

Also commonly detected are the rovibrational lines of H $_2$. Arising from levels about 6000 K above the ground state, these lines trace hot molecular gas. While the diagnostic use of these lines is complicated by the fact that multiple excitation mechanisms can play a role (and probably do play a role), such as fluorescence following UV-absorption, shock waves and X-ray excitation, they provide a unique high-resolution probe of molecular gas in galactic nuclei which can often be used for gas-dynamical studies.

In addition to these emission features, there are photospheric absorption features arising in the cool atmospheres of red supergiants created in the starburst. These include the CO first overtone absorption bands at 2.30 μm and longer wavelengths, as well the second overtone absorptions in the *H*-band; there are also atomic absorption lines (e.g., SiI 1.59 μm , NaI 2.21 μm and CaI 2.27 μm) which together with the CO bands can be used for stellar dynamical studies as well as for spectral typing of the dominant stellar population.

Finally, high-excitation so-called coronal lines (named after their detection from the solar corona) require a hard radiation

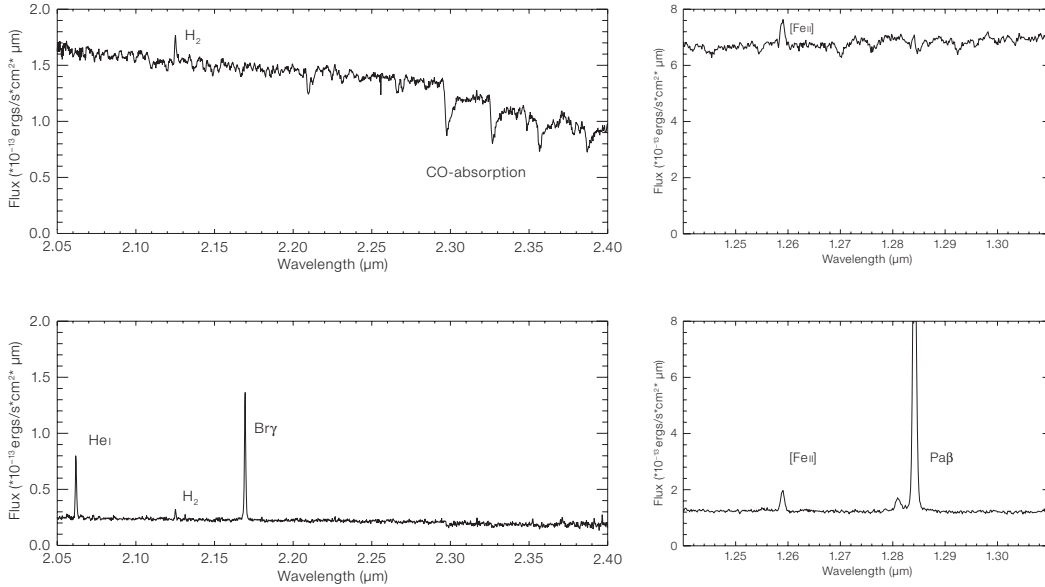


Figure 4: SINFONI spectra taken at two positions in M83. Shown are SINFONI K-band spectra (left column) and partial J-band spectra (right column) on the K-band continuum peak (upper panels), on the peak of the Br γ emission (lower panels). These spectra are from Vermaas et al. (in preparation).

field that cannot be produced by normal young stars and therefore reveal the presence of an active galactic nucleus (AGN); these lines include [SiVI] 1.96 μm , [CaVII] 2.32 μm and [SiX] 1.25 μm .

With the exception of the coronal lines, all of these lines are evident in the spectra shown in Figure 4. Given that these tracers probe different temporal phases of the starburst, they can be used as an age indicator. For instance, the Br γ equivalent width EW(Br γ) can be formed by dividing the Br γ emission by the underlying continuum, thus measuring the relevant importance of young O-stars and their direct descendants, the red supergiants, which is time-dependent and can thus be used to determine the age of the stellar population. Age determinations may also be obtained by comparing Br γ flux to CO absorption bands (again a comparison of O-stars with red supergiants) or [FeII] flux (O-stars compared to supernova remnants). Turning again to Figures 3 and 4, it is seen that at the K-band nucleus the EW(Br γ) is very low, but that the CO bands are quite prominent, showing that this region is dominated by an evolved stellar population. In contrast, the bright Br γ region seen in Figure 3 has essentially no counterpart in the K-band continuum and its high EW(Br γ) thus indicates a very young age. This is also seen in its J-band spectrum, where the Pa β line is much stronger than the [FeII] line at 1.26 μm .

Since the supernova rate is dominated by stars with a mass of about 8 M_{\odot} (the most numerous stars still producing supernovae), which have a lifetime of about $3 \cdot 10^7$ years, the Br γ and [FeII] emission trace phases of the starbursts that are temporally separated by this amount of time. In principle, one could use these results then to calculate the speed at which the star formation propagates through the nuclear region. Remarkably however, there is no pattern in the derived ages. Instead, the results point to a situation in which a large area becomes globally unstable, after which individual star-forming complexes form stochastically. There is thus no evidence for propagating star formation in this region. However, a *global* trigger is still needed. Presumably this may be found in the accumulation of gas in the barred potential in the M83 nucleus, which continues until a critical value is reached, after which star formation is ignited stochastically.

Inspection of Figure 3 also reveals that the PAH emission traces star formation only approximately. Clearly the brightest PAH emission traces the brightest Br γ emission, and there is therefore no evidence for PAH destruction by the hottest stars. However, diffuse PAH emission is present also where no Br γ emission is found, e.g., in the region of the K-band nucleus. The presence of [FeII] emission in this area indicates the presence of supernova remnants, but direct excitation

by these is unlikely, given the lack of detailed morphological agreement. The presence of supernova remnants however indicates a radiation field dominated by the most massive stars that do not end as supernovae, i.e., mid-B-type stars or later. This result confirms earlier claims that PAHs can be excited by a fairly soft radiation field (e.g., Li and Draine 2002). A quantitative analysis will be able to show what fraction of the PAH emission is excited by stars of various types, which will ultimately lead to a more secure calibration of PAH emission as a star formation indicator.

Mid-IR emission as a star formation indicator

A fundamental result from Spitzer is the use of 24 μm dust emission (well away from solid state spectral features) as a star-formation indicator (e.g., Calzetti et al. 2005, Pérez-González et al. 2006). Ground-based imaging in the Q-band spectral window (17–26 μm) allows us to examine the dust emission in this spectral region in detail in spatially resolved starbursts.

An example is presented in Figure 5, where we present images of Br γ emission (from SINFONI) together with the Q-band dust emission imaged with VISIR (Snijders et al., in preparation). It is evident that these two match quite well.

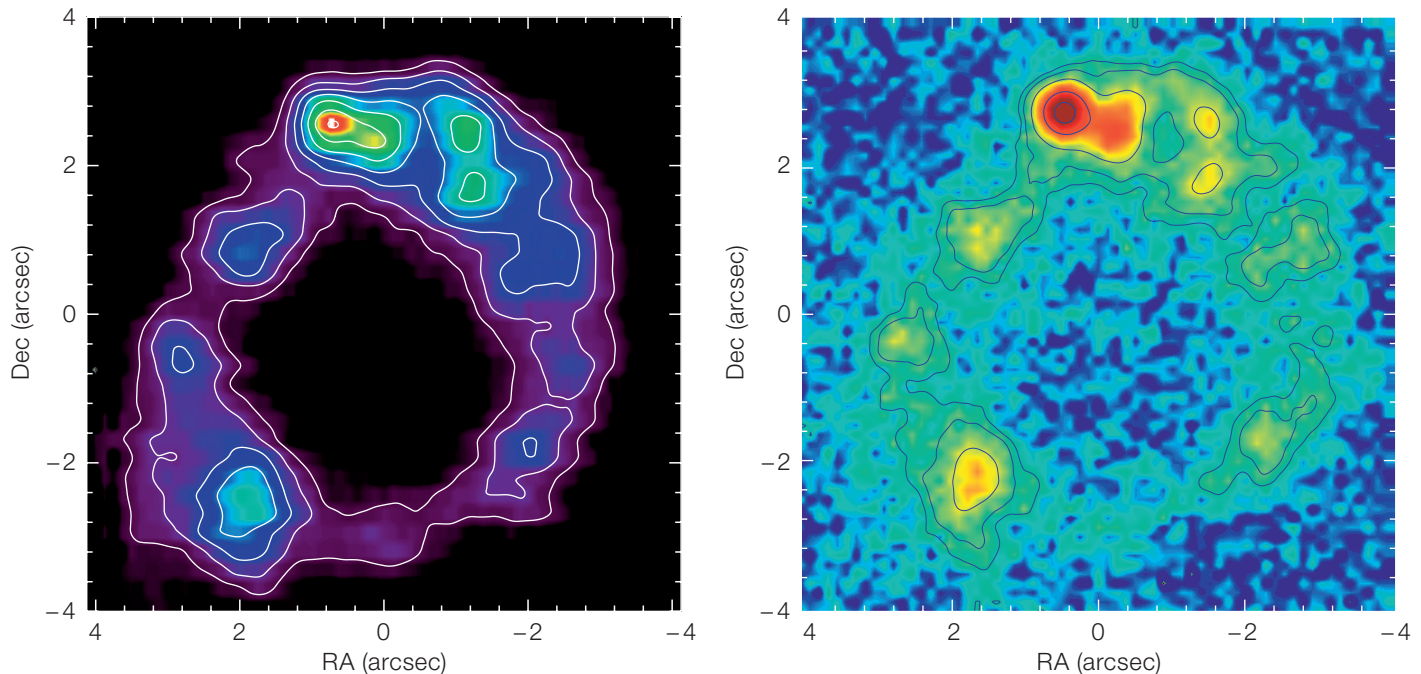


Figure 5: The circumnuclear starburst in NGC 7552. Each of these frames shows an $8'' \times 8''$ (800 pc diameter) region. **Left panel:** Br γ emission (from SINFONI); **right panel:** Q-band dust emission from VISIR; (from Snijders et al., in preparation).

These data will allow us to correlate the extinction-corrected (using the Br γ /Pa β ratio) Br γ emission with the Q-band dust emission at high spatial resolution to study both the correlation and possible deviations from the correlation (Snijders et al., in preparation).

Outlook

In this paper we have only scratched the surface of the possibilities offered by SINFONI and VISIR for ground-based studies of starburst galaxies. We are currently extending this work in two directions.

First, we are including studies of AGNs. In gas-rich galactic nuclei containing a (dormant) supermassive black hole the triggering of activity may be related to the supply of fuel to the very centre. In galaxies with an Inner Inner Lindblad Resonance (IILR) this supply is halted by a torque barrier at the IILR. In other words, under only the effects of gravity the inflowing gas will accumulate at the IILR and form a ring, which, after building up sufficient surface density, will form stars, as observed in NGC 7552 (Figure 5). However, the gas cannot pass the IILR, and any supermassive black hole located at the nucleus remains fuel-starved

and thus dormant. On the other hand, in galaxies with an active AGN, gas emission is observed all the way to the nucleus. This is the case for instance in Cen A, which has no IILR, and where our SINFONI data reveal a warped disc of H $_2$ gas, extending all the way to the nucleus. Kinematic modelling of this disc then provides a new determination of the black hole mass (Neumayer et al., in preparation).

A second avenue for expanding this work is with studies of ULIRGs. Given the now well-documented correlation of (stellar) spheroid mass with mass of the central supermassive black hole for galaxies (e.g., Magorrian et al. 1998), the formation of the bulk of the stellar mass and of the black hole must be related. It is likely that this relation is put into place in high- z ULIRGs, where violent star formation not only builds up significant stellar mass, but where an AGN is often also evident. Local ULIRGs can be studied as analogues of these high- z objects. Again, spatial resolution is essential, and with the Laser Guide Star Facility on UT4 of the VLT, it is likely that SINFONI will play a key role in revealing the nature of the relation between starburst and AGN in these extreme objects.

In summary, it is clear that with SINFONI and VISIR, and with the spatial resolution offered with the VLT and the Laser Guide Star Facility, new territory is being opened for the study of activity (starburst or otherwise) in galactic nuclei, which is not available with present space-based facilities.

References

- Calzetti D. et al. 2005, ApJ 633, 871
- Li A. and Draine B. T. 2002, ApJ 572, 232
- Magorrian J. et al. 1998, AJ 115, 2285
- Mirabel F. et al. 1998, AA 333, L1
- Pérez-González P. G. et al. 2006, ApJ 648, 987
- Snijders L. et al. 2006, ApJ 648, L25
- Wang Z. et al. 2004, ApJS 154, 193